Principal Investigator (Last, First, Middle): ROSS, ANN H.

# Geometric Morphometric Tools for the Classification of Human Skulls

**2005-MU-BX-K078**

**Ann H. Ross, Ph.D., Principal Investigator**

**Dennis E. Slice, Ph.D.**

**Shanna E. Williams, Ph.D.**

## ABSTRACT

The proposed project developed population-specific classification criteria and associated software to assist forensic scientists in the characterization of human skulls. Such tools would be an important component both in criminal investigations and in general preparedness for mass fatality incidents. These tools were incorporated into the new and powerful methods of geometric morphometrics that address significant shortcomings in traditional approaches to biological shape analysis, which are not yet widely used in forensic identification. The project objectives are three-fold: 1. To compile an extensible population database derived from three-dimensional landmark coordinate data of human cranial material that will aid in future victim identifications; 2. Develop and validate population-specific procedures for the classification of unknown individuals; 3. Develop cross-platform software for the use in forensic applications of human identification.

For this project, 3D coordinates of 75 craniofacial landmarks were collected from existing skeletal collections of European, African, and Hispanics totaling approximately 1000 individuals for use as reference data for modern populations. The x,y, and z coordinates of each landmark will be collected using a *Microscribe 3DX*® and *G2X*® digitizer. The potential for augmenting this data set with information from clinical medical images were also investigated.

Raw coordinate data are not directly comparable as shape variables to compare specimens since each set is collected in its own coordinate system. The data must be translated and rotated to a common coordinate system and scaled to a common size. To undertake these transformations a generalized Procrustes analysis approach will be used that minimizes the sum of squared distances between landmarks of each skull and those of an iteratively-computed

mean. The resulting shape variables will then be used to develop group-specific multivariate classifications.

The software provides a classification of an unknown specimen into a probable sex and ancestral affiliation with one or more likely populations including allowances for fragmentary and damaged specimens. Initial development focused on the characterization of Hispanics of different geographical origins and their morphological relationships with groups of European and African ancestry, but the resulting tools will be easily extensible to other groups. The various aspects of the research were presented to the forensic community at the American Academy of Forensic Sciences conference, which have resulted in several publications in the Journal of Forensic Sciences.

## TABLE OF CONTENTS

**Page**

**Abstract** 1

**Executive Summary** 3

**Technical Proposal**

I. Statement of the Problem 6

Literature Review 7

II. Materials and Methods 11

Anticipated Characterization and Classification 17

Software Development 22

Summary 23

III. Results 24

IV. Conclusions

1. Discussion of Findings 40

2. Implications for Policy and Practice 44

3. Implications for further research 44

V. References Cited 45

VI. Dissemination of Research Findings 49

**Appendix**

**Craniofacial Landmarks** **51**

**Executive Summary**

The estimation of sex and ancestry are key components when rendering a biological profile from skeletal or otherwise unidentifiable remains. The estimation of sex and ancestry are critical first steps in a biological profile, as other elements in the analysis of human skeletal remains, such as age and stature, are sex and ancestry specific and cannot be adequately determined without this information. The precise estimation of sex and ancestry are also critical in the identification process as they can narrow the search of an unknown individual, which can lead to identification and final disposition of the remains. The proposed work involved the development, verification, and implementation of new geometric-morphometric-based technologies relevant to the identification of human remains to aid the investigative process. We compiled a database (N = 1086) composed of craniofacial three-dimensional landmark coordinate data that will aid in future victim identifications and integrate this information into task-specific software for the assignment of membership probabilities in previously defined sex and ancestral groups to unknown remains. The results of this research have been and will continue to be reported at forensic conferences (e.g. American Academy of Forensic Sciences, NCSU Forensic Science Symposium) and peer-reviewed literature, and the core software, 3D-ID, developed as part of this project will be made available to the forensic and research communities. The software can be downloaded from the web (http://www.3d-id.org/index.html). The specific goals of the project were:

1. Compile a reference database (extensible to include new data from groups not specifically incorporated in the initial research) for the analysis of coordinate data in forensic applications of human identification.

2. Develop and validate population-specific methods and formulae for the classification of unknown individuals based on the state-of-the-art of methods of geometric morphometrics.

3. Develop and make widely available easy-to-use, cross-platform classification software, including comprehensive documentation and training/tutorial material, for use by forensic and other investigators and students.

## I. Introduction

### 1. Statement of the Problem:

A key component to expediting the identification process is the ability to most accurately determine race or ancestral information from skeletal remains. The knowledge of the ancestral origins of an individual drastically narrows the search for missing persons, and this can ultimately increase the speed and likelihood of successful victim identification and facilitate the reconstruction of the events surrounding a crime.

At present, only minimal quantitative osteological analyses are performed to estimate race or ancestry in the purely clinical setting (Ross et al. 1999, 2002; Ross and Kimmerle 2009). The collection and analysis of more comprehensive skeletal information using advanced technology and data analysis methods is seldom undertaken. This is in spite of the fact that modern methods are available that address a number of potentially serious shortcomings in the methods underlying traditional analyses. This project addresses this problem by providing new, easy-to-use, non-invasive, and non-destructive tools that incorporate state-of-the-art methods consistent with the most current, yet mature theory of shape analysis for the forensic classification of skeletal remains. The project specifically focuses on skulls, as they are the most commonly used skeletal elements used in population studies because they are known to be more genetically driven and less affected by environmental factors such as nutrition (Sparks and Jantz 2002; Ross and Ubelaker in press; Ross and Kimmerle 2009; Kimmerle et al. 2008). In addition, this research will help to verify the evidentiary reliability of determining sex and ancestry from human skeletal remains in keeping with the court rulings of *Daubert v. Merrell Dow Pharmaceuticals, Inc* (509 US.579, 1993) that requires methods to be published in peer-reviewed

publications and have associated known or potential error rates admissible as evidence in court proceedings.

2. **Literature citations and review**

*Traditional Methods*

Since the 1960's, forensic anthropologists have utilized their knowledge of population variation to develop measurement standards and discriminant functions to estimate ancestry from human remains (Giles, 1964; Giles and Elliot, 1962; Ubelaker et al., 2002). In the mid- 1980's, Richard Jantz from the University of Tennessee created the Forensic Data Bank (NIJ grant # 85-IJ-CX-0021) using traditional techniques of size and shape analysis based on linear measurements to assemble skeletal data to improve identification methods (Jantz and Moor-Jansen, 1988; Moore-Jansen et al, 1994). This effort resulted in the computer program FORDISC 3.0 (Ousley and Jantz, 1996) that is widely used by forensic practitioners and derives custom discriminant functions for up to 21 cranial measurements to classify unknown crania into 7 possible racial groupings (White, Black, Amerind, Japanese, Hispanic, Chinese, and Vietnamese) dependent on the sex of the individual. The utility of the software is dependent upon the similarity of the unknown skull to one of the reference populations within FORDISC (Ubelaker et al., 2002).

Historically, methods of size and shape analysis, such as those employed by FORDISC, have relied on the application of multivariate statistical methods (e.g. multivariate analysis of variance, discriminant function analysis, etc.), to sets of caliper measurements that correspond to linear distances, and sometimes to angles (Lynch et al. 1996; Rohlf and Marcus 1993; Ross et al. 1999). One of the major limitations of this type of data acquisition and analysis is that the measurements or angles are ultimately based on the positions of the endpoints, or anatomical

landmarks, by which they are defined, yet encode only incomplete information about the relative positions of these defining points (Bookstein, 1991; Slice, 2005, 2007). In many such cases, for instance, information on biological variation crucial for ancestral determination may not be conveniently oriented along the span of such caliper measurements that are commonly recorded in a traditional analysis (e.g., Ross et al., 1999).

*Geometric Morphometrics*

Modern methods of size and shape analysis, called geometric morphometrics, address the potentially serious problems of traditional methods by focusing on the analysis of landmark coordinates (Rohlf and Marcus, 1993; Slice, 2005, 2007). Such data completely and efficiently archive the geometric information available in the landmarks, and any traditional measurement based on the same points can easily be recovered using elementary geometric formulae. Furthermore, since these methods retain the geometric relationships between the points throughout an analysis, graphical depictions are possible that allow one to more easily relate the results of abstract multivariate procedures directly to the morphology of interest.

Once sets of coordinate data have been superimposed in a common coordinate system, using the method of Generalized Procrustes Analysis (GPA – methodological details of which can be found in Slice, 2005, 2007) (Rohlf and Slice, 1990; Slice, 2005, 2007), they can be treated as multivariate shape variables and subjected to familiar statistical procedures such as principal components analysis, the construction of multi-group classification functions, or canonical variates analysis. These newer morphometric methods using three-dimensional landmark coordinates can provide considerably more anatomical information than their traditional counterparts, but they have received little to no application in forensic anthropology or victim identification (Ross et al, 1999, Ross and Kimmerle, 2009).

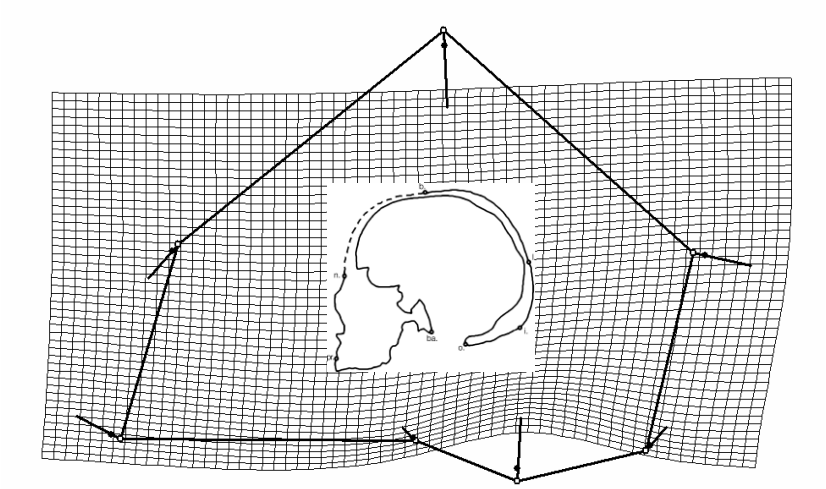

**Figure 1** Thin-plate spline and vector representation of the statistically significant difference (x5) in mean shape between the two samples. Inset indicates anatomical position of landmarks.

Figure 1 illustrates a result of such a procedure applied to 2D data. The difference in mean shape between two groups (Austrian Europeans, n=85, and Khoi-San Africans, n=34) is highly significant ($P<0.001$ based on between-group SS of 999 random permutations of group membership) and accounts for about nine percent of the total sample variation. Figure 1 illustrates this difference both as vector differences from the Austrian mean to the Khoi-San mean and as a thin-plate spline (Bookstein, 1991; see also Slice, 2005) mapping of the Austrian into the Khoi-San mean. The differences have been exaggerated by a factor of five. The figure clearly shows the main differences between the groups as being due to a relative antero-posterior lengthening of the head in the Khoi-San and a striking rotation in the relative orientation of the foramen magnum. These are "pure" shape differences since all specimens have been scaled to a standard (centroid) size (see Slice, 2005), but the original sizes have been sequestered in a separate scale parameter that can be analyzed separately. In this case, the Khoi-San crania are significantly larger on average than the Austrian crania ($P=0.002$ by randomized ANOVA with 999 permutations).

This methodology is easily extended to three-dimensional data as shown in Figure 2 of the (statistically significant) mean difference in relative landmark location of cranial landmarks in Mexican and Cuban crania. Here differences in mean landmark locations are shown as difference vectors (thin-plate splines are less effective visualization tools in 2D representations of 3D data) magnified by a factor of two.

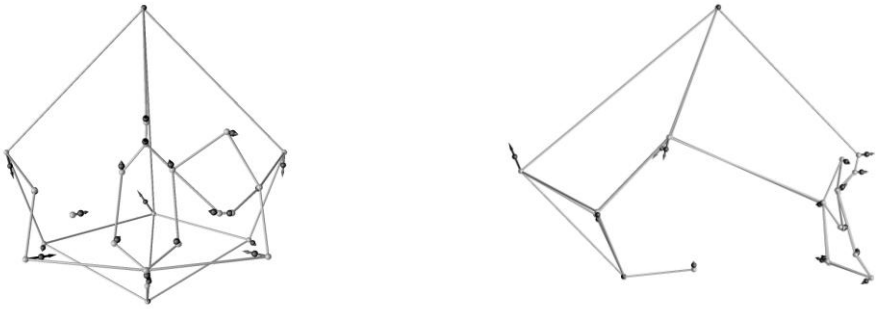

**Figure 2** Morphological differences (x2) between Mexicans and modern Cubans.

The newer geometric morphometric methods using three-dimensional landmark coordinates can provide considerably more anatomical information than their traditional counterparts, but they have received little to no application in forensic anthropology or victim identification (Ross et al, 1999; Ross et al. 2004; Ross and Kimmerle 2009). The value of these newer methods in the forensics setting is illustrated by the results of Ross and colleagues (1999), who found that while the geometric morphometry classification results for an American Black and an American White sample were comparable to traditional discriminant analysis, it outperformed traditional methods in its ability to locate specific regions of variability that would otherwise have remained undetected. In addition, because the geometric morphometry was able

to detect the specific regions of variation, individuals could be classified using a reduced set of landmarks instead of a whole suite of measurements necessary using traditional caliper methods. Using a reduced set of landmarks can also extend the utility of this method to the identification of fragmentary remains.

We do not anticipate that geometric morphometric methods will immediately replace more traditional methods, but they can be viewed as the next logical step in developing new tools for victim identification. As an added benefit, these new methods can conveniently utilize the same standard craniofacial landmarks known to most forensic scientists and can thereby address all of the shortcomings associated with the analysis of sparse linear measurements in a familiar context. Also, it is possible that the results of a comprehensive geometric morphometric analysis will be a reduced set of traditional measurements that contain most of the information about specimen affinity. However, such a conclusion would be based on the comprehensive analysis of all available geometric information and not just an incomplete sampling of that variability.

## II. Materials and Methods

Data was collected from skeletal remains with known demographics (e.g. ancestry, age, and sex) from national and international forensic laboratories and museums. In addition, we re-evaluated currently used ancestral classifications to improve correct allocations of unknown individuals. As such, present day classifications systems do not necessarily have biological meaning. For example, the term "Hispanic" includes all Spanish speaking peoples and does not adequately address the distinct ethnohistorical origins of the populations and it is a biologically meaningless term (Ross et al. 2004). South American populations are very distinct from Central American populations and from Spaniards from Spain. To address these shortcomings we

divided our reference populations into geographic regions represented by closely related populations (e.g. Mesoamerican, Circumcaribbean, South American, European American, European, etc.). Although there is still much variation within each region, these groupings better address the biological similarities and differences among these closely related populations. In addition, as European Americans are an amalgamation of numerous European groups we did not group them together with European individuals from Europe. The same holds true for individuals of African origin. It will be an ongoing process to locate underrepresented groups such as Asians, Central Americans, Puerto Ricans, etc., which will be included in the database as they become available. Given the nature of collecting data from skeletal remains, to name a few such as known demographics, skeletal incompleteness, poor preservation, trauma and pathology that hide the necessary landmarks, the anticipated sample size was approximately 700 individuals. However, we were able to surpass this initial estimate and our reference database includes 1089 individuals, which will increase as newly acquired samples are included (see Table 1 for sample composition). Only trauma and pathology free individuals were included in the reference population. The reference sample was amassed from various national and international museum collections and laboratories and from many researchers kind enough to provide their data for this endeavor. Museum collections included in this project are: Maxwell Museum in Albuquerque, Samuel Morton Collection at the Penn Museum, University of Pennsylvania (http://penn.museum/documents/publications/expedition/PDFs/50-3/renschler.pdf), American Museum of Natural History, NY, Luis Lopes Collection at the Bocage Museum in Lisbon, Portugal (see appendix for collection information), Oloriz Collection in Spain (http://www.ucm.es/info/museoana/Colecciones/Craneos/index_english.htm), Juan Munizaga Collection curated at the Universidad de Chile, The Donated Collection at the University of

Tennessee, Knoxville, C.A. Pound Human Identification Laboratory at the University of Florida, Morgue Judicial, Republic of Panama, North Carolina Office of the Chief Medical Examiner, and the Georgia Bureau of Investigation.

| **Table 1. Sample Composition** | **Total sample N = 1089** | |
|---|---|---|
| African: unknown (n = 16) | African: female (n = 5) | African: male (n = 6) |
| African American: female (n = 123) | African American: male (n = 149) | Circumcaribbean: female (n = 4) |
| Circumcaribbean: male (n = 22) | East Asian: female (n = 2) | East Asian: male (n = 9) |
| European: unknown (n = 90) | European: female (n = 59) | European: male (n = 71) |
| European American: female (n = 134) | European American: male (n = 238) | Historic African American: Female (n = 1) |
| Mesoamerican: unknown (n = 1) | Mesoamerican: female (n = 8) | Mesoamerican: male (n = 35) |
| South American: unknown (n = 3) | South American: female (n = 35) | South American: male (n = 44) |
| Unknown: unknown (n = 10) | Unknown: female (n = 3) | Unknown: male (n = 18) |

The positions of a maximum of 75 standard, homologous craniofacial landmarks were recorded for each skull to reflect the among-group variation (see Appendix). Although, a

maximum of 75 landmarks will be collected not all will be used in the various analyses. As part of this project, we sought to identify the landmark subsets that can best discriminate between the groups and methods will be developed to include the analysis of fragmentary or damaged specimens as might be found in forensic investigations. It takes approximately 30-40 minutes per skull to collect the coordinates, which includes setting up the digitizer, selecting specimens, and marking the Type 3 landmarks with a pencil prior to digitization. The landmark definitions will follow Howells (1973). A *Microscribe 3DX*® and *G2X*® digitizer will be used to obtain the x,y,and z coordinates for each landmark using the software *Three-Skull*, written by Stephen D. Ousley. The coordinates are obtained by placing the digitizer's stylus on the cranial landmarks and depressing the foot pedal, which records the position of the stylus tip (or x, y, and z coordinates) to a separate file.

Geometric morphometric methods are excellent candidates to utilize new sources of data to better characterize the types of population variation that could facilitate identification. For instance, while dental records and radiographs are frequently used in the forensic setting (e.g. Atkins and Potsaid, 1978; Brown et al., 1952; Ubelaker, 1984; Woolbridge, 1981) almost no use has been made of data from medical imaging modalities such as Computed Tomography (CT) scans. Such scans, based on x-rays, can be used to image soft-tissue in three dimensions, but they are particularly good at imaging bony structures such as the skull (Figure 6). CT scans can attain resolutions of 1mm or less, but are used more often to produce images with spatial resolutions (limited by slice thickness) on the order of 3 to 5mm. These clinical images may make up for any deficiency in resolution by their quantity as dozens to thousands are produced each day within a given geographical region – many of which are trauma and pathology free. In addition, data from clinical CTs also would have the advantage of being up to date and contemporary. This is

potentially important since significant secular changes have been documented in the cranial morphology in the U.S. over the past 150 years (e.g., Angel, 1976, 1982; Jantz, 2001; Jantz and Meadows Jantz, 2000; Wescott and Jantz, 2001, 2005; Kimmerle and Jantz, 2005).

To investigate the potential of such data to enhance forensic identification, coordinate data from 50 CT scans were obtained from the University of Pennsylvania Open Research Scan Archive (formerly Penn Cranial CT Database-http://plum.museum.upenn.edu/~orsa/ORSA/Welcome.html) to construct a preliminary comparative sample that will be compared to the digitized coordinates of the same skulls. To the extent possible given the differences in resolution, comparable data from the CT scans will collected using the software package, Avizo® (Visualization Science Group – http://www.vsg3d.com/vsg_prod_avizo_standard.php), and the appropriateness of including such data in our reference database will be examined. Should such data prove suitable, clinical images could provide a far larger source of contemporary information than the current somewhat limited and "aging" skeletal collections.

As part of our standard research protocol, we will carry out a repeatability study in which multiple observers digitize a group of skulls multiple times in random order. Replicate measurements will then be examined using appropriate statistical tests such as MANOVA and ANOVA to identify significant effects of cranium (expected), observer, and their interaction. Though universally ignored, recent research (Slice et al., 2004) has shown such interactions are part of cranial digitizing and even include a landmark interaction term in which different landmarks on different skulls are differentially difficult for individual observers. Our landmark set and collection protocol will be modified to account for the results of this investigation.

The coordinate data will be processed using the established methods of geometric morphometrics to produce suites of shape variables to be used in the construction of dynamic allocations rules for classifying an unknown individual (see below) and used as the reference material by the software to be developed in the course of this project.

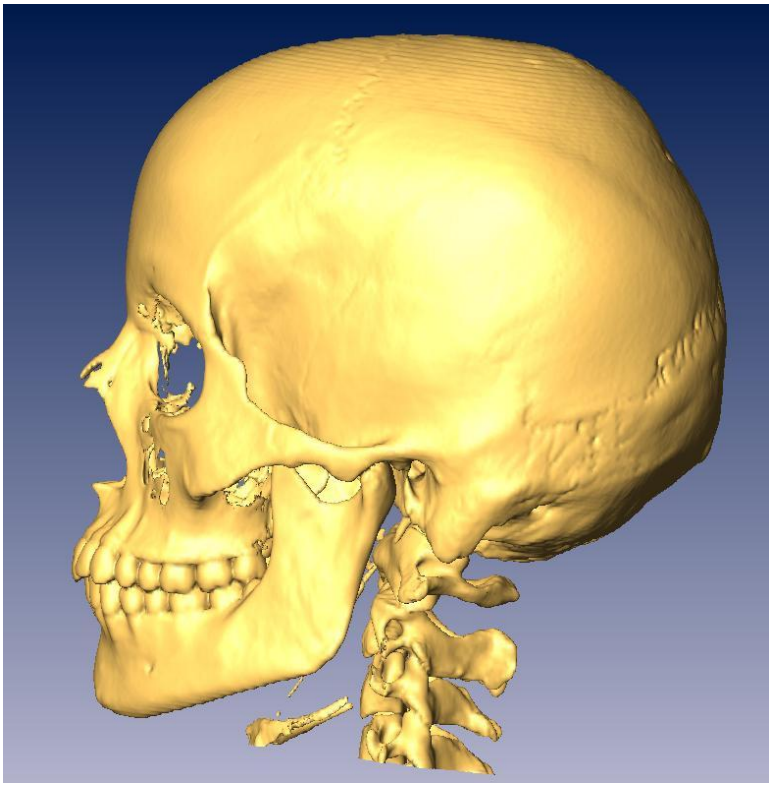

**Figure 6** Skull surface and other bony surfaces extracted from a clinical CT scan of a 21 year-old European female. Note the sutures, protuberances, foramina, and individual bones used to define many standard craniometric landmarks. X,Y,Z resolution of source scan is 0.7x0.7x1.25mm.

**Anticipated Characterization and Classification**

Two important objectives of this project were to determine whether the geometric morphometric characterization of the patterns of craniometric variability within populations will be relevant to forensic identification in the United States and also to develop classification methods and tools for the assignment of unknown or unidentified individuals. In the classic classification problem, individuals of unknown group affiliation are assigned to predefined groups in order to minimize the classification error adjusted for posterior probabilities of group membership, as well as the cost functions associated with such misclassification (Johnson and Wichern, 2002). For two populations, the general formulation is to mathematically define regions, $R_i$, such that

$$R_1: \quad \frac{f_1(\mathbf{x})}{f_2(\mathbf{x})} \geq \left(\frac{c(1|2)}{c(2|1)}\right)\left(\frac{p_2}{p_1}\right)$$
$$R_2: \quad \frac{f_1(\mathbf{x})}{f_2(\mathbf{x})} < \left(\frac{c(1|2)}{c(2|1)}\right)\left(\frac{p_2}{p_1}\right),$$

where $f_i(\mathbf{x})$ is the density function of the *i*th population evaluated at the data vector **x** (in our case, superimposed landmark coordinates), $c(i \mid j)$ is the cost of misclassification of a member of group *j* as a member of *i*, and the $p_i$ are the prior probabilities of membership in group *i*. We do not feel that the cost of misclassification in the forensic setting should be asymmetrical across ethnic groups, and furthermore, we believe it is inappropriate to distinguish amongst alternatives for determining prior probabilities, although such prior information could be considered in the final assignment of group membership. For example, the proportion of the local population or the

proportion of victims apportioned to ethnic groups. Using equal cost functions and prior probabilities in the above equation simplifies to:

$$R_1: \quad \frac{f_1(\mathbf{x})}{f_2(\mathbf{x})} \geq 1$$
$$R_2: \quad \frac{f_1(\mathbf{x})}{f_2(\mathbf{x})} < 1$$

Relatively simple classification rules for assigning an unknown individual to one of a number of ancestral groups can be derived from the above equation assuming, for instance, multivariate normal populations with homogeneous co-variance structure. In that case, one assigns the unknown to population *i* for which the linear discriminant score,

$$\hat{d}_i(\mathbf{x}) = \bar{\mathbf{x}}_i \mathbf{S}_{pooled}^{-1} \mathbf{x} - \frac{1}{2} \bar{\mathbf{x}}_i^t \mathbf{S}_{pooled}^{-1} \bar{\mathbf{x}}_i$$

is the largest, where $\mathbf{S}_{pooled}$ is the pooled within-group estimate of the covariance matrix of the $i^{th}$ group and $\bar{\mathbf{x}}_i$ is the mean data vector for that sample. Extensive use of geometric morphometrics, specifically generalized Procrustes analysis, suggests that the assumption of multivariate normality can be reasonable, despite the Reimannian nature of GPA space (Slice, 2001). Equality of co-variance structure is less likely, in which case, one should use a quadratic allocation rule for assigning the unknown to the group that maximizes

$$\hat{d}_i^Q(\mathbf{x}) = -\frac{1}{2} \ln|\mathbf{S}_i| - \frac{1}{2} (\mathbf{x} - \bar{\mathbf{x}}_i)^t \mathbf{S}_i^{-1} (\mathbf{x} - \bar{\mathbf{x}}_i),$$

where $\mathbf{S}_i$ is the sample covariance matrix for the $i^{th}$ population. Both of the above rules minimize the estimated total probability of misclassification when their respective assumptions hold true.

There are several situations that arise both within the general classification problem, as well as with its specific application to geometric morphometric data sets. First, while the above equations are formulated to minimize the total probability of misclassification when the assumptions hold true, this is not necessarily reflective of the rules performance when it is based on sample estimates and applied to future unknowns. In order to evaluate this aspect of the rules performance, one must either divide the data set into two and use one, the training data set, in constructing the algorithm and classifying the members of the other, the test data set, to get an actual expected error rate. This is wasteful of the data, so a preferable approach is the "holdout" or cross-validation method of Lachenbruch and Mickey (1968), where an expected error rate is computed based on the individual classification of each of the *n* specimens using rules generated by the other $n - 1$ observations. This validation will help fulfill, in part, the requirements of *Daubert v. Merrel Dow Pharmaceutical, Inc.*, which mandates the admissibility and reliability of expert scientific evidence that valid scientific methods have a known or potential error rate.

Data dimensionality is another issue in the application of geometric morphometrics within the context of classification. The above equations utilize the inverse of the group or the pooled within-group co-variance matrix. The existence of this inverse is minimally dependent upon having more (preferably many more) observations than variables. Yet, comprehensive geometric morphometric data sets usually include a large number of variables: the number of landmarks, *p*, multiplied by the number of dimensions, *k*. For instance, with $p = 75$ landmarks in $k = 3$ dimensions subjected to Generalized Procrustes Analysis, one has $p \times k = 75 \times 3 = 235$

variables. Initially, we will not have this many observations for any group and for some groups, it is possible that we will never have this many observations. Subsequently, the constraints on location, orientation, and scale imposed by the superimposition ensure that the co-variance matrix of the complete set of superimposed coordinates will be singular, regardless of sample size, because for 3D the actual dimensionality of the scatter will be, at most, $p \times k - 7$ (see Slice, 2005). These general features of Procrustes analysis can be addressed in several ways. For the usual types of significance testing (group differences, regression, etc.) that similarly rely on co-variance matrix determinants or inversions, non-parametric methods are the preferred solution.

For this project, we will employ dimension reduction techniques to construct linear combinations of the observed variables that meet the computational requirements of the classification rules. The most reasonable approach is that of Principal Components Analysis (PCA), which provides the best (in a least-squares sense) low-dimensional representation of the data. Specifically, we will use the first few Principal Components (the number to be determined by sample size and inspection of sample co-variance structure) as the variables for the classification. These can be generated using pooled co-variance matrices if the ancestral or ethnic groups were found to be sufficiently homogenous in co-variance, or on a group-by-group basis if pronounced heteroscedasticity is present. In the latter case, the implications for classification are unknown and will be investigated as part of the proposed research.

Finally, the dependency of the co-variance structure on the variables is an issue unique to geometric morphometrics. In the current proposal, the variables are the Procrustes superimposed coordinates of anatomical landmarks. Unlike traditional variables in which the co-variance structure of a subset of variables can be computed by simply striking out rows and columns of the co-variance matrix for the entire data set, the co-variance matrices of subsets of Procrustes

coordinates must be computed anew, starting at the superimposition stage. Since material may be fragmentary, this is particularly relevant to the identification of human remains in the forensic context. In addition, while ante-mortem trauma or pathology can potentially be important in final personal identification, it will negatively impact the classification procedure and thus, should be excluded. Therefore, our system will allow for the re-computation of classification rules using the comparative database and the data (landmark coordinates) available from the unknown individual.

**Software Development**

The dynamic construction of classification rules based on the reference data collected in the course of this project will be implemented in a stand-alone, Java-based program. Java is a widely-used, platform-independent language that is well-supported by most common operating systems, including Microsoft Windows, Linux and other versions of unix, as well as Mac OS X. This cross-platform capability is possible since Java programs are "interpreted" at runtime by a platform-specific "virtual machine." This interpretation introduces an additional layer of program execution that carries with it some performance penalty, but given the speed of today's computers, this should not be a significant (or even noticeable) problem for the data sets to be collected in the course of this project or any future extension thereof.

Basic program operation will involve the investigator entering the three-dimensional coordinates (or missing data codes) for specific landmark locations on an unknown specimen into the software program. The program will then construct a generalized-Procrustes-aligned sample of the reference data allowing for missing data in the unknown specimen, compute classification functions for each group in the reference collection in the resulting alignment, fit

the unknown configuration to the grand mean of the superimposed reference data, compute scores for membership of the unknown in each group based on the quadratic allocation rule, and generate a report including relevant information for the unknown data (group name, missing values, etc.) and ordered membership scores for each group. Expanded and updated reference data sets will be made available to users as they are accumulated in the course of future research and checked for accuracy and precision. Subsequent versions of the software could easily be made to allow end users to enhance or add their own reference samples, and we will establish repeatability criteria based on our own work to ensure the ongoing quality of the reference database and assist end users in developing their own (See Results section for actual methods used for characterization and classification).

**Summary**

To summarize, we will:

- Collect craniofacial landmark coordinate data for ancestral groups relevant to the classification of unknown human remains within the United States forensics community.
- Subject this data to generalized Procrustes analysis to assess co-variance structure.
- Use the above results to generate statistical classification rules and test the expected actual misclassification rate for complete data sets.
- Implement and investigate methods for the reduction of data dimensionality for use in the above rules.
- Implement and investigate procedures for classification of unknowns with missing data.

- Develop and distribute the software and reference databases necessary for the use of these methods by workers in the forensics community. Such software will produce a most-likely assignment of an unknown to one of the available reference groups, provide quantitative summaries of alternative assignments, and produce appropriate graphical output and commentary so that investigators can assess the reliability of an individual assignment.
- Maintain and distribute updated databases that include new data from individuals of known demographic and ancestral affiliation.

## III. Results

*Actual Characterization and Classification*

Several approaches to the classification of an unknown were examined in the development of 3D-ID (See Anticipated Characterization and Classification section). Initially, we implemented classification algorithms in which superimpositions, dimensionality reduction, and co-variance matrix estimation were carried out on a group-by-group basis. This seemed to be the approach with the least assumptions about homogeneity of the within-sample co-variance structure and with the least influence by other groups on the computed similarity of the unknown to a specific group.

Initial testing showed this approach did not yield classification rates that we thought were acceptable, despite their sophistication and arguable superiority. Thinking this might be the result of the separate fitting of the unknown to each group, we implemented an algorithm in which the superimposition step was carried out for all groups simultaneously to an iteratively estimated grand mean, while individual, within-group covariance matrices were still used in the

computation of the Mahalanobis distance from the unknown to the group mean. Dimensionality reduction was also carried out on a within-group basis. While this approach brought improved classification, it was still deemed insufficient for practical use. As a result, the third and least sophisticated method was employed. In this method, the superimposition is carried out simultaneously to the grand mean of all reference specimens. Dimensionality reduction is based on a total principal components analysis and Mahalanobis distances computed using the pooled, within-group co-variance matrix (a practice that assumes homogeneity of within-group variation patterns and magnitudes). Again, this improved the rate of classification, but still not to the degree we had anticipated.

It was ultimately determined that the failure of the simplest method was due to the poor handling of ill-conditioned co-variance matrices at a very low level. The addition of checks to identify and deal with this situation resulted in substantial improvements in correct classification rates. So, in its initial release, 3D-ID implements the third approach to classification (simultaneous superimposition, overall PCA for dimension reduction, and pooled, within-group co-variances). We anticipate that future versions will include the "backing out" of our classification scheme and the transition to the new, more robust methods in simultaneous superimposition and within-group PCAs and co-variance estimation. Details of the allocation algorithm follow.

Upon initiation of processing, the three-dimensional coordinates are parsed and checked for validity. If acceptable, the reference database is scanned and any specimens lacking any of the landmarks for which data were provided for the unknown are removed. Then, each object in the data structure, including the unknown, is purged of landmarks for which no data has been provided from the unknown.

Next, the remaining reference data set is subjected to a generalized Procrustes superimposition in which all specimens (regardless of group) are fit to an iteratively computed grand mean. The unknown is then separately fit to the grand mean using ordinary Procrustes analysis. If the "Include size" option has been selected, size is restored to the reference data and unknown by multiplication of the coordinates by the inverse of the standardizing scale factor used in the Procrustes superimposition. The coordinate data of the superimposed reference sample is then subjected to a principal components analysis and the reference data and (superimposed) unknown projected onto the requisite number of shape dimensions. At all stages, checks are made to ensure the dimensionality of the available data is compatible with the requested shape dimensions and minimal sample size per dimension.

At this point, we have compatible reference data Procrustes superimposed along with the unknown data into a reduced-dimension shape space. From here on, the classification involves computations identical to those that would be used for non-coordinate data. Group means and the pooled, within-group co-variance matrix is computed. Coordinate differences are computed between the unknown and each group mean, and these are converted to Mahalanobis squared distance, $D^2$:

$$D_k^2 = (\mathbf{u} - \bar{\mathbf{x}}_k)\mathbf{S}_{pooled}^{-1}(\mathbf{u} - \bar{\mathbf{x}}_k)^{\mathrm{t}}$$

Where **u** is the row vector of the unknown's coordinates projected into the reduced shape space, $\bar{\mathbf{x}}_k$ is the row vector of mean coordinates for group *k* in the same space, and $\mathbf{S}_{pooled}$ is the pooled, within-group co-variance matrix.

The suggested allocation is based on the group to which the unknown has the smallest $D^2$. Following the predictive approach outlined by Campbell (1985), posterior probabilities and typicalities are computed to assess the degree to which the proximity of the unknown to a particular group mean is distinctive and the degree to which the unknown is likely to be found amongst true members of a particular group. Posterior probabilities are computed for individual groups by:

$$P\left(\mathbf{u} \mid \bar{\mathbf{x}}_k, \mathbf{S}_{pooled}\right) = \pi^{-v/2}\Gamma\left(\left(n_f+1\right)/2\right)\Gamma\left(\left(n_f-v+1\right)/2\right)^{-1}\left|n_k^{-1}\left(n_k+1\right)n_f\mathbf{S}_{pooled}\right|^{-1/2}\left(1+n_k\left(n_k+1\right)^{-1}n_f^{-1}D_k^2\right)^{-\left(n_f+1\right)/2}$$

where $v$ is the number of shape dimensions, $n_f$ = total reference $n$ – the number of groups, $n_k$ is the size of the $k^{\text{th}}$ group, and $\Gamma$ is the gamma function. Typicality for the $k^{\text{th}}$ group is computed from

$$v^{-1}\left(n_f-v+1\right)n_f^{-1}\left(n_k+1\right)^{-1}n_kD_k^2 \sim F\left(v, n_f\right)-v+1$$

*Cross-validation study*

The flexibility of the software and the classification approach allows the maximum number of individuals to be considered for construction of the reference populations with no a priori limitation on the specific landmarks (out of the primary landmark list) available for a specimen. Thus, reference samples can be constructed for any specimen with data available for any subset of the primary data list. This flexibility, however, causes problems in the assessment of classification success, as different mixtures of individuals, landmarks, and parameters lead to different results that might not be directly comparable. To address this, a separate reference

dataset was constructed from the main reference data set. Specimens with numerous missing coordinates were deleted. The remaining specimens were examined and several landmarks that were frequently missing were selectively marked as missing in all specimens. Thus, we have a reference data set of 897 individuals, all with data for the same 30 of the 35 original reduced set of landmarks (see results section for landmark reduction and repeatability study). Furthermore, one landmark, inferior nasal border, has been removed from consideration by the program, but remains in the reference databases. In this way, we have a standard, consistent database, referred to as the "trimmed" data, with which to assess the classification accuracy of the program.

The cross-validation study showed that as the number of shape dimensions increased, the correct classification rate increased, as well. However, with more-and-more required shape dimensions, the specimens from the reference sample for which a meaningful classification could be made was reduced – individuals which could only be classified into their correct group or could only be assigned to an incorrect group due to parameter constraints were excluded from consideration in the cross-validation study. The minimum number of individuals per shape dimension was kept at one for this analysis. Combining the contrasting patterns showed that the maximum number of specimens from the trimmed reference data set was classified correctly at a specified shape dimensionality of 53. This resulted in 77% of 692 individuals being correctly classified. This result led to the use of 53 as the default shape dimension.

*Digitizing Error and Repeatability (see publication)*

Part of the purpose of this project was to evaluate the repeatability and error associated with the collection of coordinate cranial landmark data via direct digitization from dry skulls. Data capturing techniques range from direct digitization of landmarks via 3D digitizers to point extraction from scanned images. Several studies tested the precision, repeatability and validation of anthropometric landmarks from computed tomography, and other optical surface imaging methods and they were all found to be highly repeatable. However, although Richtsmeier (1995) found that CT scans were internally consistent, she cautioned against the use of CT data in combination with other direct means of measurement. These newer modalities of data acquisition and analyses have undergone little to no systematic testing for accuracy particularly from direct skull digitization.

Table 2. *Subset of landmarks used with abbreviations.*

| |
|---|
| 1. Alare left (alarl) |
| 2. Alare right (alarr) |
| 3. Bregma (brg) |
| 4. Dacryon left (dacl) |
| 5. Dacryon right (dacr) |
| 6. Euryon left (eul) |
| 7. Euryon right (eur) |
| 8. Lambda (lam) |
| 9. Metopion (met) |
| 10. Occipital subtense point (ocspt) |
| 11. Opisthocranion (opg) |
| 12. Parietal subtense point (paspt) |
| 13. Radiometer point left (radptl) |
| 14. Radiometer point right (radptr) |
| 15. Subspinale (ssp) |
| 16. Zygion left (zygl) |
| 17. Zygion right (zygr) |
| 18. Zygoorbitale left (zygool) |
| 19. Zygoorbitale right (zygoor) |

Nineteen standard homologous cranial landmarks were collected using a Microscribe 3DX and G2X ® digitizer and the software ThreeSkull written by Steve Ousley (Table 2). The landmarks were chosen to include those standard landmarks frequently taken as well as standard caliper derived anatomical points. Three skulls were randomly selected for this study from the C.A. Pound Human Identification Laboratory. Each skull underwent three separate digitization sessions by two separate observers for a total of six digitizations for each skull. Ideally, you would want to acquire the coordinate data from the skulls fixed in a particular coordinate system between digitizing sessions. However, in this study the skulls were digitized at two separate locations-by Shanna at the C.A. Pound Human ID Lab and then by me at NC State. In this case,

a Generalized Procrustes Analysis is not recommended as any error due to repeatability would be masked by the "fitting" process or the process of translating and rotating the raw coordinate data into a common coordinate system and scaling it to a common size.

Because the skulls were not "fixed" in a common coordinate system between digitizing sessions, interlandmark linear distances (ILDs) were used in the subsequent statistical analysis rather than the landmark coordinates. All possible ILDs between the nineteen landmarks (n = 171) calculated as N(N-1)/2 for N landmarks for each digitizing session (n = 3) for each observer (n = 2) for each skull (n = 3) were calculated using the program PAST (Paleontological Statistics, 2001, http://folk.uio.no/ohammer/past/download.html).

Digitization error (proportion of the total variance explained by multiple digitizing sessions of the same skull) was tested using a mixed model analysis of variance (ANOVA) with the ILDs as dependent variables. Thirty-two percent or 54 out of the 171 ILDs showed error due to digitizing in excess of five percent of the total variance observed (Table 3).

Repeatability defined here as the between-observer variation- was tested with ANOVA using the general linear model (GLM) routine. The GLM procedure detected significant between-observer difference for fourteen interlandmark distances (Table 4). Table 4 shows that the landmarks that are not highly repeatable are those involving the type three landmarks, specifically, euryon, alare, and radiometer point. In addition, parietal and occipital subtense points seem to be problematic. However, these may reflect the differential acquisition of these points as one observer used a coordinate caliper to locate the points prior to digitization, while the second observer used contour data to calculate the points. Interestingly, three of the interlandmark distances with significant between-observer variation had endpoints on dacryon and two with endpoints on Zygoorbitale. Occasionally these landmarks may be difficult to locate

especially if they are ill defined due to suture obliteration, which may be reflect the present results.

The GLM procedure revealed significant observer-by-session difference for thirteen interlandmark distances (Table 5). These results are consistent with the between-observer difference results presented in the previous slide in that the majority includes ILDs with Type 3 landmarks, specifically euryon, alare, opisthocranion and radiometer point. In other words, the observers are having difficulty locating type 3 landmarks across digitizing sessions for the same skull. Interestingly, opisthocranion seems to be more problematic across different sessions of the same skull than between observers.

Extremal or type 3 landmarks such as euryon are fairly accurate when instrumentally derived as linear distances in traditional morphometrics. However, these results demonstrate that they are highly variable when attempting to archive their exact anatomical location and are associated with a sizeable degree error, both between and within observers. Thus we caution the use of Type III landmarks and recommend utilizing only types 1 and 2 landmarks, which are considered biologically significant, in geometric morphometrics

Table 3. *ILDs showing >5% error (see Table 2 for landmarks).*

| | **Observer** | **1** | **Observer** | **2** |
|---|---|---|---|---|
| **ILD** | Min | Max | Min | **Max** |
| **1 (1-2)** | 23.88 | 27.59 | 23.99 | **27.26** |
| **2 (1-3)** | 139.12 | 151.42 | 139.53 | **150.16** |
| **5 (1-6)** | 117.43 | 136.98 | 108.91 | **126.24** |
| **6 (1-7)** | 123.18 | 138.52 | 129.45 | **139.18** |
| **8 (1-9)** | 95.50 | 106.98 | 96.31 | **107.20** |
| **10 (1-11)** | 162.32 | 193.40 | 164.09 | **188.57** |
| **13 (1-14)** | 97.40 | 107.07 | 96.52 | **105.03** |
| **17 (1-18)** | 39.60 | 47.33 | 39.90 | **48.22** |
| **22 (2-6)** | 128.62 | 145.21 | 119.36 | **136.48** |
| **23 (2-7)** | 109.78 | 126.14 | 115.41 | **126.07** |
| **27 (2-11)** | 160.86 | 192.05 | 165.44 | **187.11** |
| **30 (2-14)** | 85.89 | 95.82 | 86.19 | **93.90** |
| **31 (2-15)** | 16.79 | 19.48 | 18.46 | **20.00** |
| **34 (2-18)** | 21.87 | 26.99 | 17.10 | **24.61** |
| **37 (3-5)** | 105.83 | 115.20 | 104.75 | **114.39** |
| **38 (3-6)** | 79.17 | 122.03 | 91.58 | **101.36** |
| **43 (3-11)** | 125.47 | 146.10 | 115.90 | **143.15** |
| **53 (4-6)** | 94.61 | 125.75 | 90.26 | **107.86** |
| **54 (4-7)** | 102.15 | 120.10 | 111.69 | **118.30** |
| **55 (4-8)** | 151.38 | 176.84 | 151.98 | **175.58** |
| **56 (4-9)** | 66.45 | 71.15 | 61.70 | **70.79** |
| **57 (4-10)** | 148.93 | 170.98 | 149.12 | **174.01** |
| **58 (4-11)** | 149.83 | 17761 | 151.45 | **175.38** |
| **61 (4-14)** | 91.35 | 100.41 | 93.86 | **99.55** |
| **63 (4-16)** | 67.35 | 77.19 | 68.03 | **73.32** |
| **67 (5-6)** | 106.97 | 132.37 | 102.19 | **118.19** |
| **68 (5-7)** | 87.09 | 109.72 | 96.46 | **108.78** |
| **76 (5-15)** | 43.21 | 52.63 | 43.41 | **52.12** |
| **80 (5-19)** | 67.31 | 75.06 | 68.55 | **73.00** |
| **81 (6-7)** | 115.47 | 134.18 | 115.50 | **132.60** |
| **82 (6-8)** | 71.98 | 106.18 | 91.27 | **105.54** |
| **83 (6-9)** | 92.81 | 139.35 | 97.40 | **116.43** |
| **89 (6-15)** | 130.59 | 147.87 | 121.10 | **142.13** |
| **91 (6-17)** | 95.42 | 122.36 | 87.67 | **110.40** |
| **92 (6-18)** | 124.89 | 142.72 | 118.52 | **135.30** |
| **94 (7-8)** | 90.33 | 114.51 | 87.37 | **105.41** |
| **97 (7-11)** | 96.29 | 116.44 | 86.54 | **110.83** |
| **100 (7-14)** | 47.51 | 65.49 | 40.92 | **59.54** |
| **101 (7-15)** | 124.04 | 145.92 | 128.99 | **143.80** |
| **102 (7-16)** | 131.31 | 146.50 | 131.47 | **142.84** |
| **103 (7-17)** | 120.18 | 140.38 | 127.40 | **137.34** |
| **105 (7-19)** | 51.38 | 69.02 | 50.21 | **63.69** |
| **108 (8-11)** | 16.74 | 45.85 | 22.52 | **34.03** |
| **114 (8-17)** | 159.41 | 187.42 | 160.06 | **186.66** |
| **118 (9-11)** | 152.65 | 185.24 | 144.14 | **183.87** |
| **127 (10-11)** | 1.49 | 49.81 | 14.98 | **20.25** |
| **129 (10-13)** | 79.69 | 97.84 | 79.87 | **105.24** |
| **136 (11-12)** | 83.54 | 102.36 | 80.16 | **97.11** |
| **139 (11-15)** | 166.42 | 203.42 | 173.44 | **197.65** |
| **140 (11-16)** | 119.60 | 149.18 | 127.06 | **148.45** |
| **141 (11-17)** | 153.97 | 186.33 | 156.94 | **182.75** |
| **157 (14-15)** | 98.77 | 109.34 | 98.50 | **107.07** |
| **159 (14-17)** | 101.24 | 109.81 | 102.30 | **108.49** |
| **167 (16-18)** | **95.42** | **107.39** | **93.97** | **105.80** |

Table 4. *Between-observer variation*

| ILD | DF | Type III SS | MS | F Value | Pr>F |
|---|---|---|---|---|---|
| Alarl-dacr | 1 | 3.89 | 3.89 | 29.98 | 0.03 |
| Alarl-brg | 1 | 36.38 | 36.38 | 70.85 | 0.01 |
| Alarr-paspt | 1 | 63.13 | 63.13 | 19.39 | 0.05 |
| Brg-radptl | 1 | 13.23 | 13.23 | 27.03 | 0.04 |
| Dacl-radptl | 1 | 5.05 | 5.05 | 24.24 | 0.04 |
| Dacl-zygool | 1 | 6.02 | 6.02 | 22.78 | 0.04 |
| Dacr-zygool | 1 | 6.14 | 6.14 | 233.91 | 0.004 |
| Eul-radptl | 1 | 196.67 | 196.67 | 167.09 | 0.006 |
| Eur-lam | 1 | 111.36 | 111.36 | 44.53 | 0.02 |
| Eur-ocspt | 1 | 700.79 | 700.79 | 36.1 | 0.03 |
| Met-ocspt | 1 | 71.72 | 71.72 | 29.98 | 0.03 |
| Paspt-radptr | 1 | 9.93 | 9.93 | 20.01 | 0.05 |
| Paspt-ssp | 1 | 50.97 | 50.97 | 69.64 | 0.01 |
| Ssp-zygool | 1 | 0.58 | 0.58 | 30.88 | 0.03 |

Table 5. *Observer*session variation.*

| ILD | DF | Type III SS | MS | F Value | Pr>F |
|---|---|---|---|---|---|
| Alarl-opg | 2 | 10.05 | 5.02 | 4.54 | 0.05 |
| Alarr-ssp | 2 | 1.15 | 0.58 | 5.15 | 0.04 |
| Brg-opg | 2 | 46.33 | 23.16 | 6.91 | 0.02 |
| Dacl-ocspt | 2 | 4.25 | 2.12 | 17.13 | 0.001 |
| Eurl-opg | 2 | 53.76 | 26.88 | 14.51 | 0.002 |
| Eurl-paspt | 2 | 7.15 | 3.57 | 7.55 | 0.01 |
| Eurl-radptr | 2 | 19.74 | 9.87 | 5.11 | 0.04 |
| Lam-opg | 2 | 120.29 | 60.15 | 6.08 | 0.03 |
| Met-opg | 2 | 13.85 | 6.93 | 8.31 | 0.01 |
| Ocspt-zygool | 2 | 3.78 | 1.69 | 7.99 | 0.01 |
| Opg-paspt | 2 | 118.35 | 59.17 | 6.78 | 0.02 |
| Opg-zygool | 2 | 4.74 | 2.37 | 5.79 | 0.03 |
| Zygl-zygoor | 2 | 11.28 | 5.64 | 5.05 | 0.04 |

Because of the results of this repeatability and digitizing error study, we trimmed the number and types of landmarks used in the final classification software. All 75 craniofacial landmarks continue to be collected, however, we included only Type 1 and Type 2 landmarks, which have proven to be me more repeatable and for which have shown to be more biologically meaningful. Thus, the landmark set was reduced to 34 (see appendix for list of reduced set of landmarks). Figures 7-10 depict the reduced set of landmarks used in the software 3D-ID. Please see Section VI Dissemination of Research Findings for a reprint of the published article.

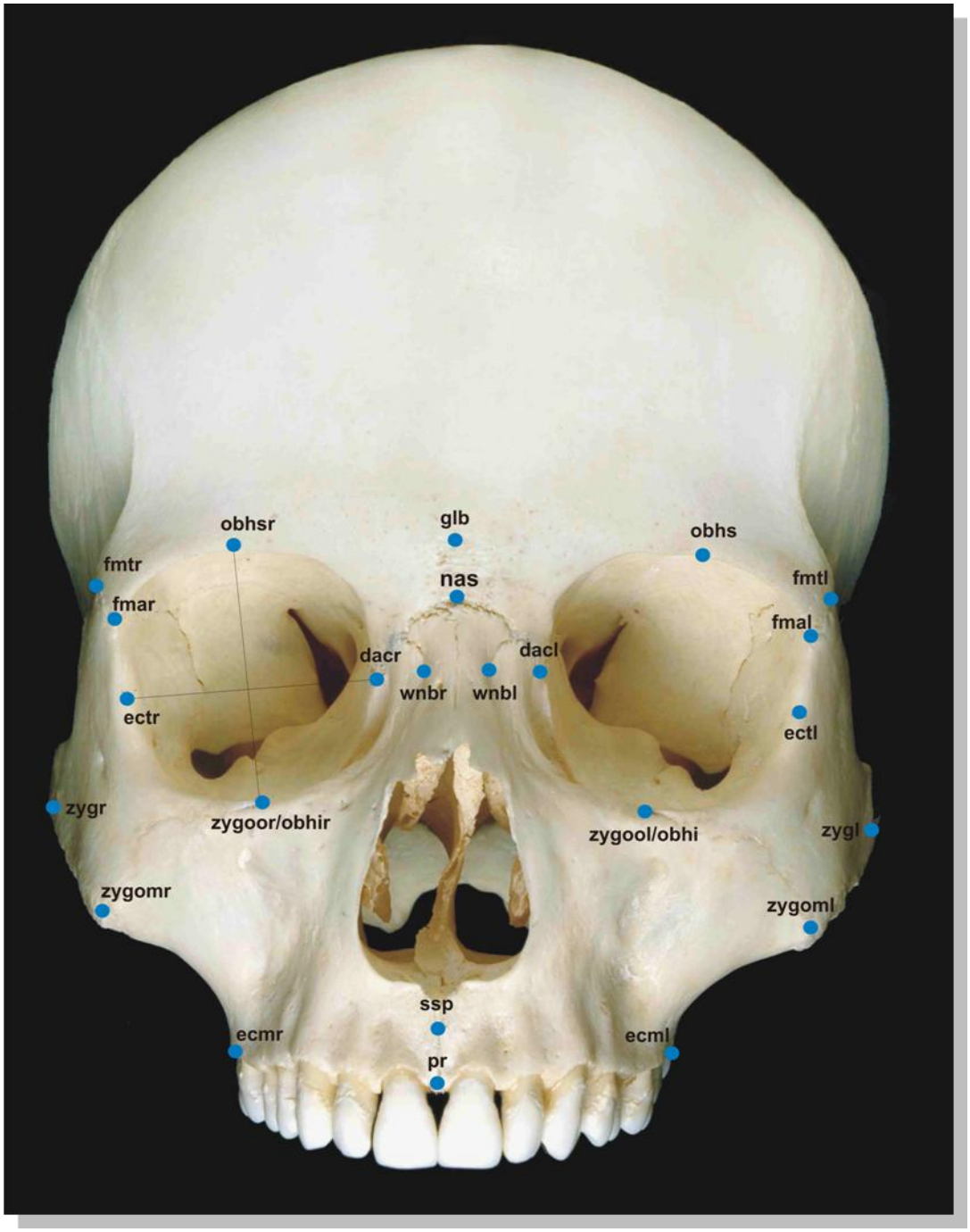


Figure 7. Reduced set of landmarks used in final software development on the anterior view of skull.

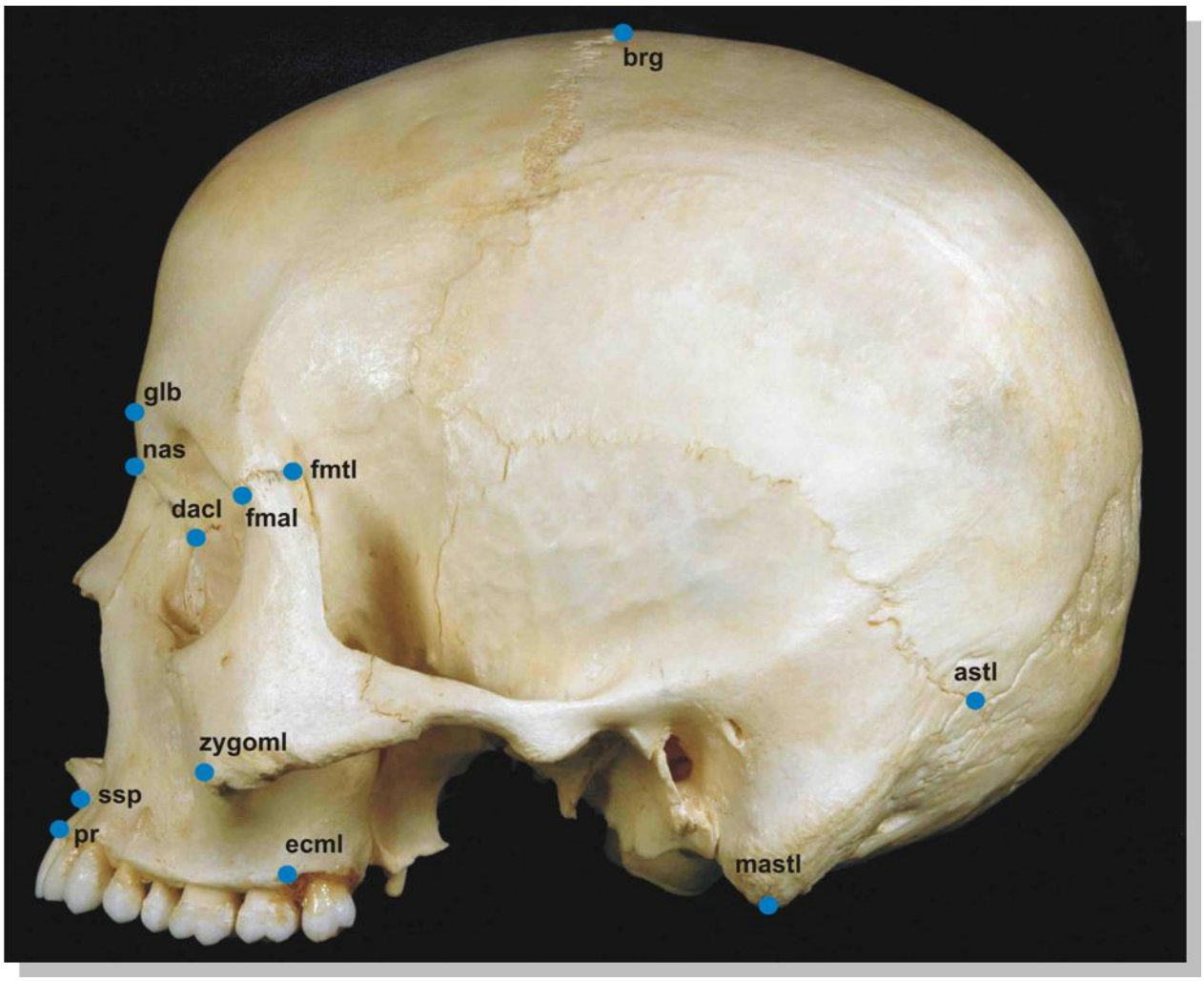


Figure 8. Reduced set of landmarks used in final software development on the lateral view of skull.

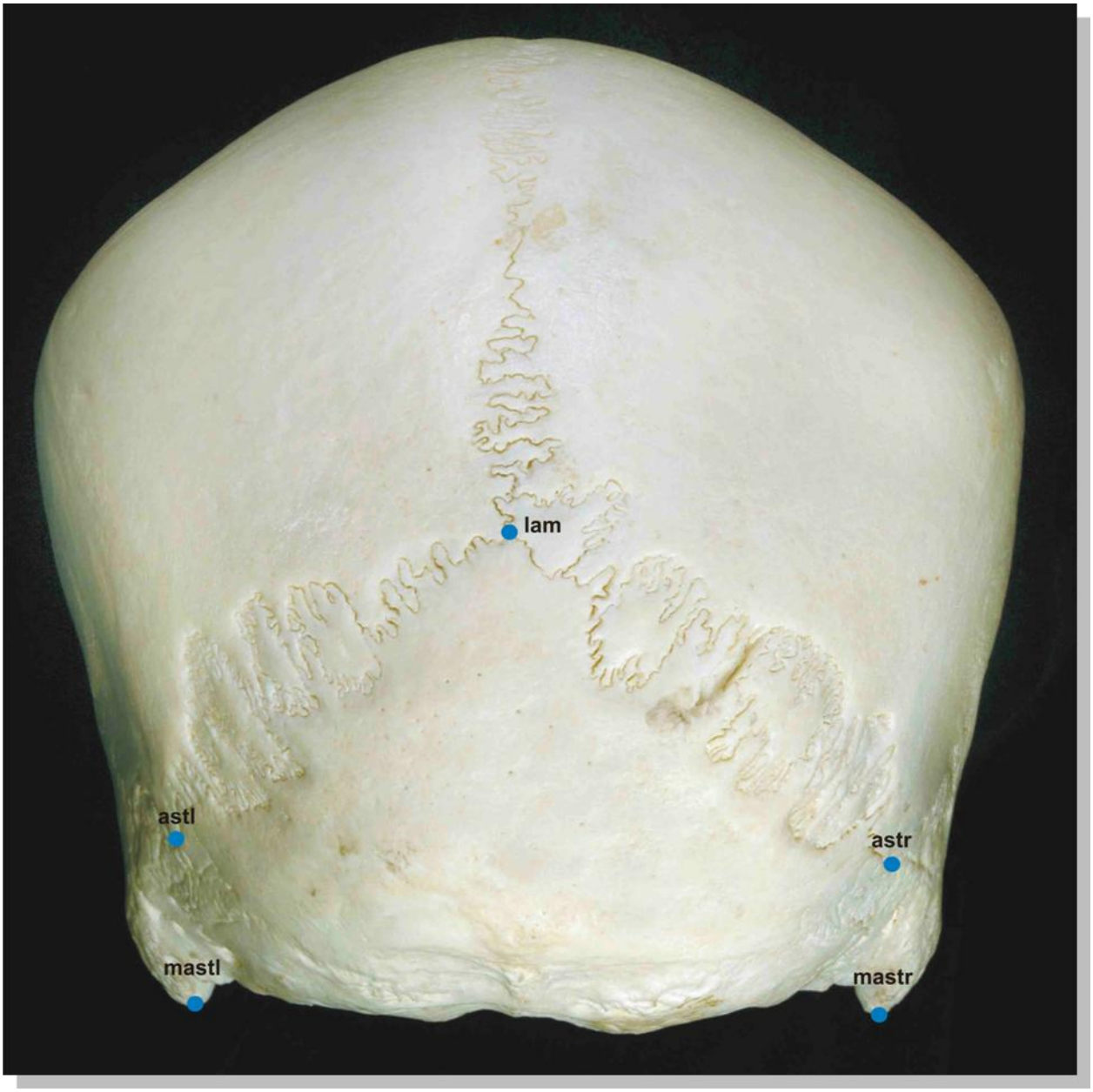


Figure 9. Reduced set of landmarks used in final software development on the posterior view of skull.

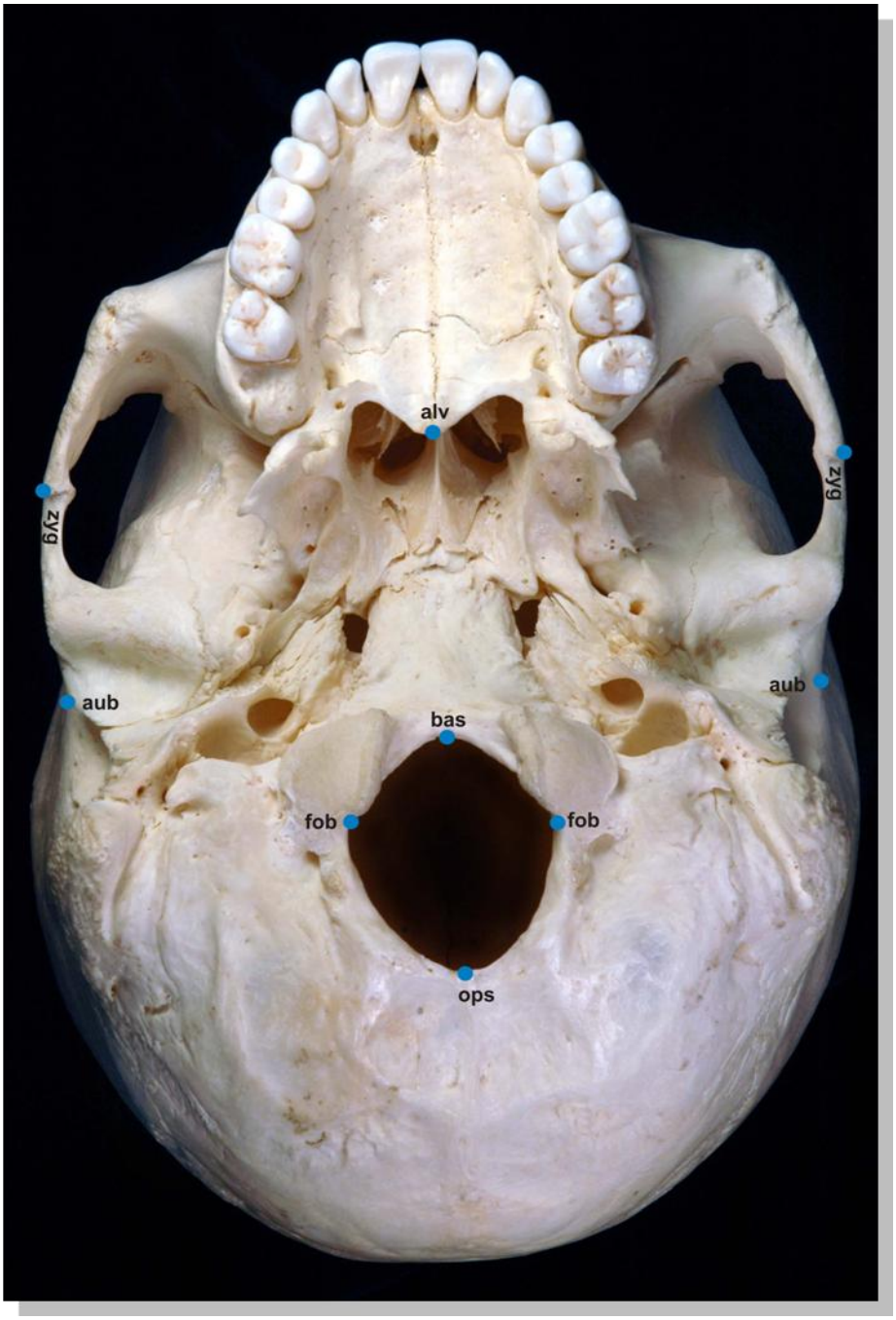


Figure 10. Reduced set of landmarks used in final software development on the inferior view of skull.

*Performance on Forensic Cases*

The PI has been utilizing the newly developed software 3D-ID in current forensic cases. The software appears to be performing well and results are comparable to those obtained with FORDISC 3.0. For example, in a recent positively identified case, 3D-ID (www.3d-id.org) classified the individual as a **European-American Male** with a posterior probability of 0.6565 and typicality of 0.3332 and FORDISC classified the individual as a **White Male** with a posterior probability of 0.775 and typicality of 0.362. Notably, our software was able to differentiate and allocate the individual as a European-American and not classify into the European group. Figure 11 illustrates the program's data input page.

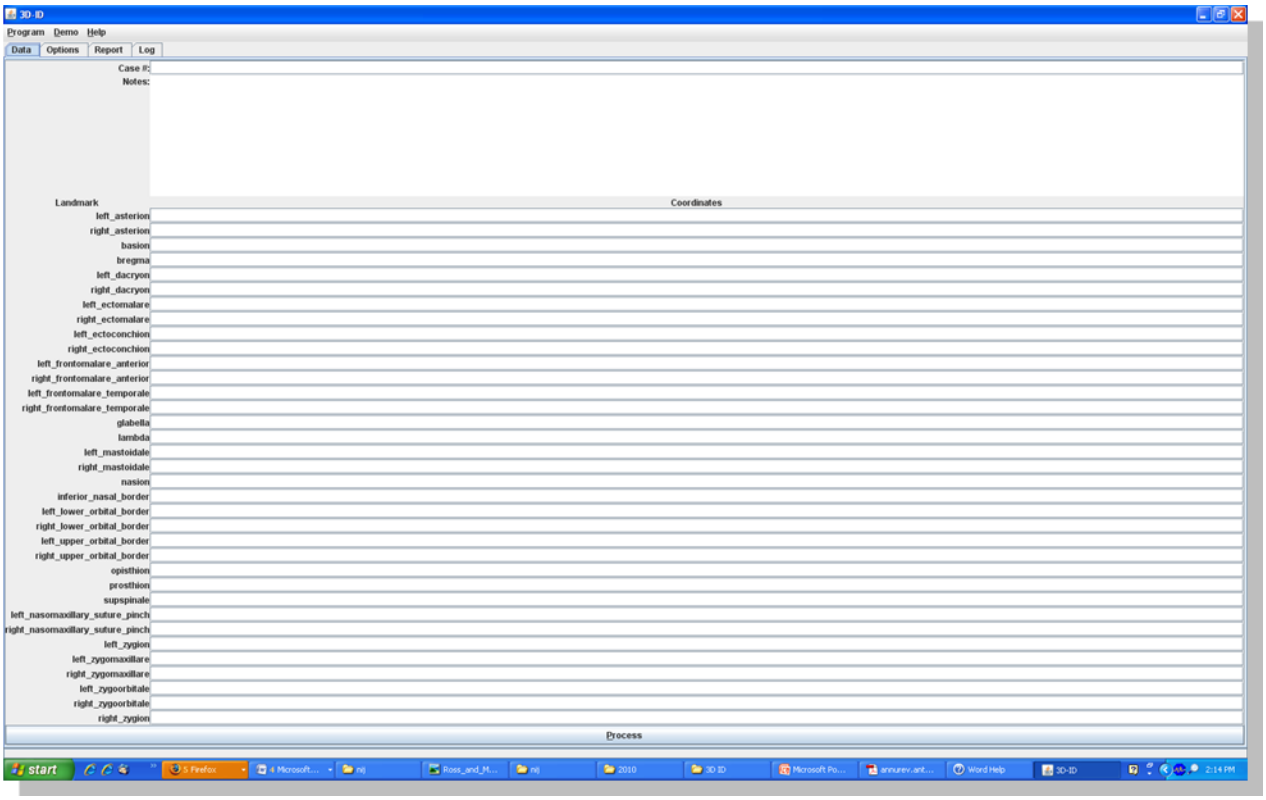


Figure 11. 3D-ID data input page.

*Examination of CT Scans as a Potential Source of Data*

Landmark data was extracted from 50 CT scans using the software AVIZO®. Thirteen craniofacial landmarks from the reduced set were selected to test whether CT scans could be a potential for data. Due to various reasons, which included landmark availability and visibility due to preservation, CT resolution and scanner bed covering landmarks, etc., 22 individuals were included in this portion of the study.

**Table 6.** *Landmarks used in CT study*.

| | |
|---|---|
| Nasion | Zygomaxillare l/r |
| Frontomalare anterior l/r | Asterion l/r |
| Subspinale | Opisthion |
| Prosthion | Basion |
| Dacryon l/r | |

Because the skulls were not "fixed" in a common coordinate system between digitizing sessions, interlandmark linear distances (ILDs) were used in the subsequent statistical analysis rather than the landmark coordinates. All possible ILDs between the thirteen landmarks (n = 78) calculated as N(N-1)/2 for N landmarks were calculated using the program PAST (Paleontological Statistics, 2001, http://folk.uio.no/ohammer/past/download.html).

A paired t-test was performed to test whether CT acquired landmarks differed significantly from the digitizer acquired landmarks. Twenty-one percent or 16 out of 78 landmarks showed a significant difference between CT acquired and digitizer acquired coordinates (Table 7).

**Table 7.** *ILD's showing significant difference between CT and digitized coordinates*.

| **ILD's** | ***p-value*** | **ILD's** | ***p-value*** |
|---|---|---|---|
| **Nas-ssp** | 0.009 | Fmar-prosthion | 0.000 |
| **Nas-zygoml** | 0.051 | Fmar-zygoml | 0.041 |
| **Nas-zygomr** | 0.041 | Fmar-zygomr | 0.033 |
| **Fmal-fmar** | 0.006 | Ssp-zygomr | 0.0424 |
| **Fmal-prosthion** | 0.000 | Prosthion-zygomr | 0.039 |
| **Fmal-zygoml** | 0.032 | Dacl-zygomr | 0.038 |
| **Fmal-zygomr** | 0.041 | Dacr-zygomr | 0.035 |
| **Zygoml-astl** | 0.036 | Zygomr-astl | 0.047 |

Some of the differences may be related to an inexperienced observer having collected the data from the CT scans. This is underscores by the errors being generally associated with Type II landmarks, which may be more difficult for an inexperienced observer to identify. Overall, however, the results show that there is no systematic bias in CT and digitizer acquired coordinates. The possibility of including data from CT scans will substantially change the composition of our forensic reference populations.

## IV. Conclusions

### *1. Discussion of Findings*

Our technology would be particularly valuable in geographic regions of the US where large ethnically diverse populations predominate. For example, in the US, the term "Hispanic" includes all persons of Spanish speaking countries. The US Census Bureau defines Hispanic or Latino as a person from Cuban, Mexican, Puerto Rican, Central or South American or other

Spanish culture of origin regardless of race. In the forensic setting, though, the use of such an umbrella term is problematic because it ignores the distinct ethnohistories and origins of each geographical population. The category for "Hispanic" used in FORDISC, for instance, combines individuals from various locations in the US, Mexico, and Central America, but mostly represents Mexican Americans. However, according to the 2002 U.S. Census, Mexicans make up sixty-six percent of the total Hispanic population in the US, while Cubans account for 3.7 percent, Puerto Ricans 8.6 percent and Central and South Americans 14.3%. Recent analysis from the Pew Research Center reveals that 40.4 million Hispanics reside in the US. This population of individuals has been historically underrepresented as a target of study in forensic scientific research. Furthermore, these different groups are more geographically concentrated in specific regions of the US and are also more likely to live in central cities of metropolitan areas than non-Hispanic whites (e.g. Mexicans in the west and the south and Puerto Ricans in the northeast). The importance of the change in these populations has been recognized by many researchers, as is evident from a session held at the 2004 Annual meeting of the American Academy of Forensic Sciences entitled, Death Investigation of Border Crossers. In all, ten (10) papers were delivered that addressed various issues including the fact that nearly 11 million undocumented individuals are in this country, 80 percent of whom are Hispanic (Falsetti et al., 2004). In addition, a recent issue of the Journal of Forensic Sciences (2008, Volume 53, Issue 1) published nine papers on "*Border Crossing Deaths*."

Both documented and undocumented persons of Hispanic background are rapidly entering the patient population of forensic scientists, and thus, the development of new tools and reference data are necessary to address this situation. In a recent study (Ross et al. 2004), we demonstrated that modern Cubans show a strong African affinity followed by a Spanish

component while lacking an indigenous Amerindian biological affinity (Figure 3). Based on known ethnohistorical origins, we predicted that Mexicans would lack the African component and would have a strong indigenous Amerindian affinity. Subsequent research (Slice and Ross, 2004; Ross et al., 2005) employing the same geometric morphometric methods used this project provided striking confirmation of this prediction (Figure 4). A result of this study is seen in Figure 2, where differences in mean landmark location are shown between Mexicans and Cubans. The Mexican crania are shown to be characterized by more lateral zygomaxillare, more inferiorly placed opisthion, more superiorly placed eurions, and more posteriorly positioned, landmarks throughout the upper face. This is in contrast to the differences seen in Figure 5, where the overall similarity of Mexicans with native populations from Ecuador is apparent in the relatively short difference vectors. The small differences between the Mexican and Ecuadorians suggest the Mexicans are characterized by infero-lateral eurions, a more medial inferior orbital border, and generally superior opisthocranion, basion, and opisthion. It is worth noting, too, that it is not just the length of the difference vectors that is relevant, but their length relative to the magnitude and direction of covariance structure at and across landmark locations, and this is taken into account in all of our procedures.

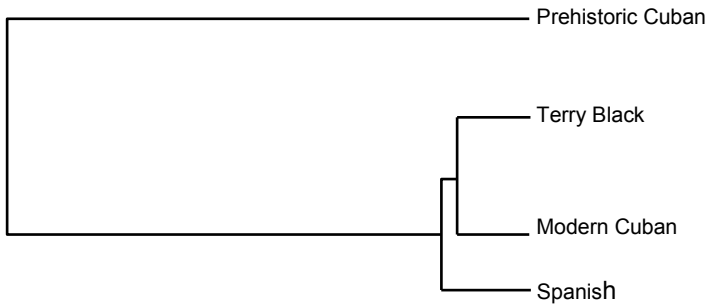


**Figure 12** Phenogram showing the morphological affinity of modern Cuban crania to modern African-American and European Spanish samples and dissimilarity of the modern and

prehistoric Cubans. Results based on UPGMA clustering of squared Mahalanobis distances between sample means computed from GPA-superimposed, three-dimensional landmark coordinates. See text for details.

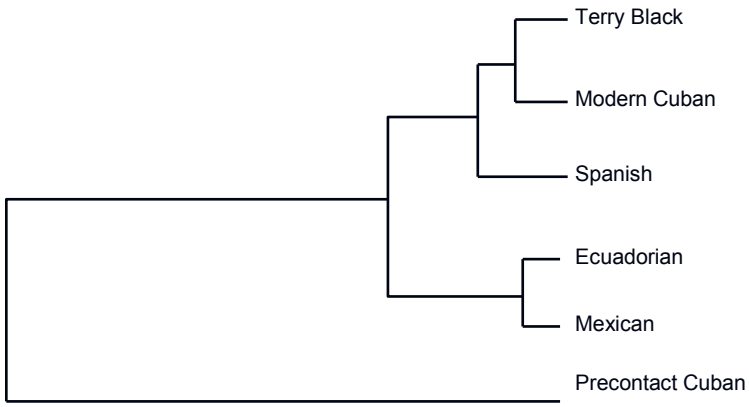


**Figure 13** Results of subsequent study (see also Fig.3) confirming predictions based on ethnohistorical considerations that modern Mexican crania would be less European and more Amerindian in morphology than Cubans – both would be considered "Hispanic" by current standards. See text for details.

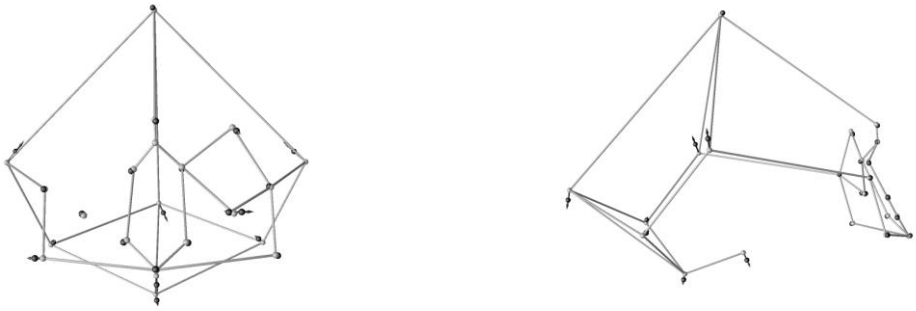

**Figure 14** Cranial differences (x2) between the morphologically similar Mexicans and native Ecuadorians. Compare with Figure 2. See text for details.

These results emphasize the need for further investigation into morphological variation in diverse populations such as Hispanics, Asians, and Native Americans. Especially in the U.S., incorporating the unique patterns of variation along with census/demographic data into forensic practice could substantially aid in the identification of unknown human remains. This project will help address this problem by providing both a reference database with more refined population subdivisions (e.g. Circumcaribbean, Mesoamerica, etc.) than are currently available and more efficient and powerful methods for the analysis of that data. In addition, this technology could extend to international identification efforts such as those currently being carried out by the Army Corps of Engineers in Iraq (e.g. discriminating between Iraqis and Kurds).

*2. Implications for Policy and Practice*

The ability of the geometric morphometry to detect the precise biological differences between commonly undifferentiated groups such as Europeans and European Americans and

Hispanics has tremendous implications in victim identifications. This is especially important in light of the changing demographics of this rapidly growing population and will assist in the identification of undocumented persons in the US. By using these modern methods along with informative prior knowledge such as census or demographic information into standard forensic practice could produce a much more informative assessment of unidentified human remains.

*3. Implications for Future Research*

Biological variation of the craniofacial region is one of the PI's major areas of research and as such, the reference population will continue to be expanded to include additional populations as they are collected. For example, in the near future we will be able to include a sample of modern Angolans in order to examine the African Diaspora in relation to morphological variation between African Americans and Africans samples from Cuba and Angola.

This technology may also be expandable to include determination of sex from the postcrania. In a recent study of the pelvis, Bytheway and Ross (In press) found sexing accuracies for European Americans of 100% for both males and females and 98% for African American females and 100% for African American males. The use of coordinate landmark data may have forensic implications for accurately being able to sex from fragmentary remains.

## V. References

Angel JL. Colonial to modern skeletal change in the U.S.A. *Am. J. Phys. Anthropol*., 1976;45:723-736.

Angel JL. A new measure of growth efficiency: skull base length. *Am. J. Phys. Anthropol*., 1982;58:297-305.

Atkins L, Potsaid MS. Roentgenographic identification of human remains. *J Am Med Ass*., 1978;240:2307-2308.

Bookstein FL. *Morphometric Tools for Landmark Data: Geometry and* Biology. Cambridge University Press, Cambridge, 1991.

Brown TC, Delaney RJ, Robinson WL. Medical identification in the "Noronic" disaster. *J Am Med Ass*.1952;148:621-627.

Falsetti AB, Walsh-Haney H, Burt MJ. Personal Identification and Death Investigation of Documented and Undocumented Migrant Workers in Florida: Demographic, Biographic, and Pathologic Factors. Pp 290. Proceedings American Academy of Forensic Sciences, Annual Meeting, Dallas, TX, 2004.

Giles E. Sex Determination by Discriminant Function Analysis of the mandible. Am J Phys Anthrop 1964;22:129-135.

Giles E, Elliot O. Race Identification from Cranial Measurements. J Forensic Sci 1962;7:147-157.

Howells WW. Cranial Variation in Man. Papers of the Peabody Museum of Archaeology and Ethnology Harvard University, volume 51, 1973.

http://www.census.gov/population/www/socdemo/hispanic.html

http://pewhispanic.org/reports/report.php?ReportID=44

http://pewhispanic.org/reports/report.php?ReportID=40

Jantz RL. Cranial change in Americans: 1850-1975. *J. Forensic Sci*. 2001;46:784-787.

Jantz RL, Meadows Jantz L Secular change in craniofacial morphology. *Am. J. Hum. Biol.* 2000;12:327-338.

Jantz RL, Moore-Jansen PH. A Data Base for Forensic Anthropology: Structure, Content And Analysis. Report of Investigations No. 47, Department of Anthropology, The University of Tennessee, 1988.

Johnson, Ronald A. and Dean E. Wichern. *Applied Multivariate Analysis*, 5th Ed. Prentice Hall, Inc. New Jersey, USA, 2002.

Kimmerle, EH and Jantz RL. 2005 (IN PRESS). Secular Trends in Craniofacial Asymmetry Studies by Geometric Morphometry and Generalized Procrustes Methods. IN Slice, D. E., ed. *Modern Morphometrics in Physical Anthropology*. Kluwer Academic Publishers, pp. 247-263.

Lachenbruch, P. A. and M. R. Mickey. Estimation of Error Rates in Discriminant Analysis. *Technometrics* 1968; 10(1): 1-11.

Lynch JM, Wood CG, Luboga SA. Geometric Morphometrics in Primatology: Craniofacial Variation in Homo sapiens and Pan troglodytes. Folia Primatol 1996;67:15-39.

Ousley SD [computer program]. Three-Skull, data acquisition software, 2004.

Ousley SD, Jantz RL. [computer program]. FORDISC 2.0. Knoxville: Department of Anthropology. The University of Tennessee, Knoxville, 1996.

Richtsmeier JT, Paik CH, Elfert PC, Cole TM, Dahlman HR. Precision, repeatability, and validation of the localization of cranial landmarks using computed tomography scans. Cleft Palate Craniofac J 1995;32:217-27.

Rohlf FJ, Slice DE. Methods for Comparison of Sets of Landmarks. Systematic Zool 1990;39:40-59.

Rohlf FJ, Marcus LF. A Revolution in Morphometrics. Tree 1993;8:129-32.

Ross AH, McKeown AH, Konigsberg LW. Allocation of Crania to Groups Via the "New Morphomtry". J Forensic Sci 1999;44:584-587.

Ross AH, Slice, DE, Ubelaker, DH, Falsetti AB. Population Affinities of 19th Century Cuban Crania: Implications for Identification Criteria in South Florida Cuban Americans, J Forensic Sci. 2004;49:11-16.

Ross AH, Slice DE, Pachar JV. Forensic Identifications and the Complexity of Determining Biological Affinities of "Hispanic" Crania. Presented at the American Academy of Forensic Sciences, 2005, New Orleans, LA.

Ross AH, Kimmerle EH. Contrubutions of Quantitative Methods in Forensic Anthropology: A New Era. In Blau, S. and Ubelaker, D. (eds.) Handbook of Forensic Anthropology and Archaeology, Humana Press, pp. 479-89.

Slice, DE. Landmark configurations aligned by Procrustes analysis do not lie in Kendall's shape space. *Syst. Biol.* 2001:50(1)141-149.

Slice, DE. Modern Morphometrics. IN Slice, D. E., ed. *Modern Morphometrics in Physical Anthropology*. Kluwer Academic Publishers, 2005:1-45.

Slice, DE, Ross AH. Population Affinities of "Hispanic" Crania. Implications for Forensic Identification. Paper presented at American Academy of Forensic Sciences, Dallas, TX 2004.

Slice, D. E., C. Unteregger, K. Schaeffer, F. L. Bookstein. Modeling the precision of landmark location data. American Journal of Physical Anthropology 2004:123(S38): 183.

Ubelaker DH. Positive identification from the radiographic comparisons of frontal sinus patterns. In Rathbun TA, Buikstra JE, editors. Human Identification: Case Studies in Forensic Anthropology. Springfield, Thomas, 1984;399-411.

Ubelaker DH, Ross AH, Graver SM. Application of Forensic Discriminant Functions to a Spanish Cranial Sample. Forensic Sci Comm 2002;4: http://fbi.gov/hq/lab/fsc/backissu/july2002/ubelaker1.htm.

Vidarsdottir U, O'Higgins P, Stringer C. A Geometric Morphometric Study of the Regional Difference in the Ontogeny of the Modern Human Facial Skeleton. J Anat. 2002;2001:211-29.

Wescott, DJ and Jantz RL. 2005 (IN PRESS). Assessing Craniofacial Secular Change in American Blacks and Whites Using Geometric Morphometry. IN Slice, D. E., ed. *Modern Morphometrics in Physical Anthropology*. Kluwer Academic Publishers, pp. 231-245.

Woolbridge, ED. Forensic dentistry. In Eckert WG, editor. Introduction to forensic sciences. Springfield, Thomas, 1981;114-154.

## VI. Dissemination of Research Findings

The results of this project have been presented at the American Academy of Forensic Sciences and several publications have been submitted to the flagship journal the *Journal of Forensic Sciences.* In addition, the methods developed in this project will be covered in Dr. Slice's courses and workshops on the geometric morphometrics. Dr. Ross also teaches several workshops a year to the forensic and law enforcement communities where she will present this new research and will incorporate the findings into the forensic sciences curriculum being developed at NC State University. The classification software, including reference database, will be distributed by the World Wide Web along with a comprehensive documentation and training/tutorial material. A modest fee and/or analysis service may be

developed to support basic maintenance of the software and the production and distribution of instructional material. The reference database will be maintained and expanded as part of ongoing and future research projects.

*Papers presented at the American Academy of Forensic Sciences*

1. A.H. Ross, D.E. Slice, J.V. Pachar. 2005. Forensic Identifications and the Complexity of Determining Biological Affinities of "Hispanic" Crania.
2. A.H. Ross, E.H. Kimmerle, D.E. Slice. 2006. What Matters- Size or Shape? Three-Dimensional Analysis of Craniofacial Sexual Variation among American Populations.
3. A.H. Ross, S.E. Williams. 2007. Repeatability and Error of Cranial Landmark Coordinates.
4. A.H. Ross, D.H. Ubelaker, E.H. Kimmerle. 2008. A Test of Methods: Implications of Dimorphism, Population Variation, and Secular Change in Estimating Population Affinity in the Iberian Peninsula.
5. S.E. Williams, A.H. Ross. 2009. Shifting Morphological Structure: Comparing Craniometric Morphology in Source and Descendant Populations.
6. A.H. Ross, S.E. Williams. 2009. Craniofacial Growth, Maturation, and Change: Teens to Midadulthood.
7. S.E. Williams, A.H. Ross. 2010. Subadult Ancestry Determinations using Geometric Morphometrics.

*Peer Reviewed Publications*

1. Slice DE. 2007. Geometric Morphometrics. *Annual Review of Anthropology* 36:261-81.

2. Kimmerle EH, Ross AH, Slice DE. 2008. Sexual Dimorphism in America: Geometric Morphometric Analysis of the Craniofacial Regions. *Journal of Forensic Sciences* 53: 54-7.

3. Ross AH, Williams SE. 2008. Testing Repeatability and Error of Coordinate Landmark Data Acquired from Crania. *Journal of Forensic Sciences* 53: 782-5.

4. Ross AH, Williams SE. 2009. Craniofacial Growth, Maturation and Change: Teens to Midadulthood. *Journal of Craniofacial Surgery* (In Press).

5. Ross AH, Ubelaker DH, Kimmerle EH. 2009. Implications of Dimorphism, Population Variation, and Secular Change in Estimating Population Affinity in the Iberian Peninsula. *Forensic Science International* (Under Review).

6. Williams S., Ross AH. 2010. Shifting craniofacial morphology between ancestral and descendant populations in the Americas. American Journal of Human Biology (Under Review).

## APPENDIX

### Original Craniofacial landmarks

| Index | Landmark | LMAbbrev | Used_for | Location |
|---|---|---|---|---|
| 1 | prosthion - Martin estimated | proM | UFHT (FDB) | MS |
| 2 | prosthion-Howells estimated | proHEST | "BPL, NPH" | MS |
| 3 | prosthion-ACTUAL | proA | | MS |
| 4 | subspinale | ssp | "SSR, SSS" | MS |
| 5 | alare L | alarl | NLB | L |
| 6 | most inferior nasal border L | nlhil | NLH | L |
| 7 | most inferior nasal border R | nlhir | NLH | R |

| | | | | |
|---|---|---|---|---|
| **8** | alare R | alarr | NLB | R |
| **9** | nasomaxillary suture pinch L | wnbl | WNB Simotic chord | L |
| **10** | nasal bone elevation | sispt | "SIS Simotic subtense, SIA" | MS |
| **11** | nasomaxillary suture pinch R | wnbr | WNB Simotic chord | R |
| **12** | deepest point on nasal bone profile | ndspt | "NDS, NDA, Gill 1b" | MS |
| **13** | zygoorbitale R | zygoor | Gill 2a | R |
| **14** | zygoorbitale L | zygool | "Gill 2a, IML, XML" | L |
| **15** | lower orbital border L/R | obhi | orbital height (inferior point) | L |
| **16** | upper orbital border L/R | obhs | orbital height (superior point) | L |
| **17** | cheek height sup point L/R | wmhs | WMH | L |
| **18** | cheek height inf point L/R | wmhi | WMH | L |
| **19** | ectoconchion L | ectl | "OBB, EKB" | L |
| **20** | dacryon L | dacl | "OBB, DKB" | L |
| **21** | dacryon R | dacr | DKB | R |
| **22** | ectoconchion R | ectr | EKB | R |
| **23** | zygion R | zygr | ZYB | R |
| **24** | zygomaxilare R | zygomr | ZMB | R |
| **25** | zygomaxilare L | zygoml | "ZMB, IML" | L |
| **26** | zygion L | zygl | ZYB | L |
| **27** | inf zygotemporal suture L | imlpt | "IML, XML" | L |
| **28** | Sup zygotemporal suture L | szs | NEW | L |
| **29** | max malar projection point L | mlspt | MLS | L |
| **30** | jugale L | jugl | JUB | L |
| **31** | marginal process lateral L | mpll | future | L |
| **32** | frontomalare temporale L | fmtl | UFBR | L |
| **33** | frontomalare anterior L | fmal | "FMB, NAS" | L |
| **34** | min frontal point L | wfbl | WFB | L |
| **35** | MAX frontal point L | xfbl | XFB | L |
| **36** | stephanion L | stpl | "STB, STS" | L |
| **37** | stephanion R | stpr | "STB, STS" | R |
| **38** | MAX frontal point R | xfbr | XFB | R |
| **39** | min frontal point R | wfbr | WFB | R |
| **40** | frontomalare anterior R | fmar | "FMB, NAS" | R |
| **41** | frontomalare temporale R | fmtr | UFBR | R |
| **42** | marginal process lateral R | mplr | future | R |
| **43** | jugale R | jugr | JUB | R |
| **44** | nasion | nas | "NOL, NLH, NAS, etc." | MS |
| **45** | glabella | glb | GOL | MS |
| **46** | supraglabellare | spglb | GLS | MS |
| **47** | metopion | met | frontal subtense and | MS |

| | | | | |
|---|---|---|---|---|
| | | | fraction | |
| **48** | bregma | brg | "FRC, BBH, PAC, PAF, PAS, etc." | MS |
| **49** | parietal subtense point | paspt | parietal subtense and fraction | MS |
| **50** | lambda | lam | "PAC, PAF, PAS" | MS |
| **51** | opisthocranion (GOL) | opg | GOL | MS |
| **52** | occiptal subtense point | ocspt | occipital subtense and fraction | MS |
| **53** | asterion L | astl | ASB | MS |
| **54** | eurion L | eurl | XCB | R |
| **55** | radiometer point L | radptl | "radii, in the middle of the EAM" | L |
| **56** | porion L | porl | MDH | L |
| **57** | mastoideale L | mastl | MDH | L |
| **58** | zyg root L | aubl | AUB | L |
| **59** | zyg root R | aubr | AUB | R |
| **60** | radiometer point R | radptr | "radii, in the middle of the EAM" | R |
| **61** | porion R | porr | MDH | R |
| **62** | mastoideale R | mastr | MDH | R |
| **63** | eurion R | eurr | XCB | MS |
| **64** | asterion R | astr | ASB | L |
| **68** | opisthion | ops | FOL | MS |
| **69** | basion | bas | "between hypobasion and endobasion. BBH,BNL," | MS |
| **70** | FOB point R | fobr | FOB | R |
| **71** | FOB point L | fobl | FOB | L |
| **72** | ectomolare L | ecml | MAB | L |
| **73** | M1 anterior point L | avrpt | AVR | L |
| **74** | ectomolare R | ecmr | MAB | R |
| **75** | alveolon (rubber band) | alv | MAL | MS |

## Reduced Suite of Craniofacial Landmarks Used in the Software

| Index | Landmark | LMAbbrev | Used_for | Location |
|---|---|---|---|---|
| **2** | prosthion-Howells estimated | proHEST | "BPL, NPH" | MS |
| **4** | subspinale | ssp | "SSR, SSS" | MS |
| **9** | nasomaxillary suture pinch L | wnbl | WNB Simotic chord | L |
| **11** | nasomaxillary suture pinch R | wnbr | WNB Simotic chord | R |
| **13** | zygoorbitale R | zygoor | Gill 2a | R |
| **14** | zygoorbitale L | zygool | "Gill 2a, IML, XML" | L |
| **15** | lower orbital border L/R | obhi | orbital height (inferior point) | L |

| | | | | |
|---|---|---|---|---|
| **16** | upper orbital border L/R | obhs | orbital height (superior point) | L |
| **19** | ectoconchion L | ectl | "OBB, EKB" | L |
| **20** | dacryon L | dacl | "OBB, DKB" | L |
| **21** | dacryon R | dacr | DKB | R |
| **22** | ectoconchion R | ectr | EKB | R |
| **23** | zygion R | zygr | ZYB | R |
| **24** | zygomaxilare R | zygomr | ZMB | R |
| **25** | zygomaxilare L | zygoml | "ZMB, IML" | L |
| **26** | zygion L | zygl | ZYB | L |
| **32** | frontomalare temporale L | fmtl | UFBR | L |
| **33** | frontomalare anterior L | fmal | "FMB, NAS" | L |
| **40** | frontomalare anterior R | fmar | "FMB, NAS" | R |
| **41** | frontomalare temporale R | fmtr | UFBR | R |
| **45** | glabella | glb | GOL | MS |
| **48** | bregma | brg | "FRC, BBH, PAC, PAF, PAS, etc." | MS |
| **50** | lambda | lam | "PAC, PAF, PAS" | MS |
| **51** | opisthocranion (GOL) | opg | GOL | MS |
| **53** | asterion L | astl | ASB | MS |
| **57** | mastoideale L | mastl | MDH | L |
| **62** | mastoideale R | mastr | MDH | R |
| **64** | asterion R | astr | ASB | L |
| **68** | opisthion | ops | FOL | MS |
| **69** | basion | bas | "between hypobasion and endobasion. BBH,BNL," | MS |
| **72** | ectomolare L | ecml | MAB | L |
| **74** | ectomolare R | ecmr | MAB | R |
| **75** | alveolon (rubber band) | alv | MAL | MS |

**Landmark Definitions for landmarks used in 3D-ID**

| Landmark | LMAbbrev | Definition |
|---|---|---|
| Left asterion | astl | Intersection of left parietal, left temporal, and occipital bones. If sutures are indistinct or include wormian bones, project suture lines until they intersect. |
| Right asterion | astr | Intersection of right parietal, right temporal, and occipital bones. If sutures are indistinct or include wormian bones, project suture lines until they intersect. |
| Basion | bas | The midline point of the anterior foramen magnum margin where it is intersected by the mid-sagittal plane. Directly opposite of the opisthion. In some cases, thickening of the margin can make position location |

| | | |
|---|---|---|
| | | difficult to determine. |
| Bregma | brg | The midline point where the sagittal and coronal sutures intersect. In cases where the intersection is interrupted, such as with fontanelle bones, the suture lines are projected. |
| Left Dacryon | dacl | Left eye orbit: point on the medial border where the frontal, lacrimal, and maxilla bones meet, also noted as the intersection of the lacrimo-maxillary suture and frontal bone. A small foramen is often present. |
| Right Dacryon | dacr | Right eye orbit: point on the medial border where the frontal, lacrimal, and maxilla bones meet, also noted as the intersection of the lacrimo-maxillary suture and frontal bone. A small foramen is often present. |
| Left Ectomalare | ecml | Left maxilla: positioned at the most lateral point on the lateral surface of the alveolar crest. Found along the second molar on the maxilla. |
| Right Ectomalare | ecmr | Right maxilla: positioned at the most lateral point on the lateral surface of the alveolar crest. Found along the second molar on the maxilla. |
| Left Ectoconchion | ectl | Left eye orbit: intersection of the most anterior surface of lateral border and imaginary horizontal line bisecting the orbit. |
| Right Ectoconchion | ectr | Right eye orbit: intersection of the most anterior surface of lateral border and imaginary horizontal line bisecting the orbit. |
| Left Frontomalare Anterior | fmal | Left side of skull: most anterior projecting point on the frontomalare suture (different from the frontomalare orbitale and temporale). |
| Right Frontomalare Anterior | fmar | Right side of the skull: most anterior projecting point on the fronto-malare suture (different from the frontomalare orbitale and temporale). |

| | | |
|---|---|---|
| Left Frontomalare Temporale | fmtl | Left side of the skull: most lateral point on fronto-malare suture |
| Right Frontomalare Temporale | fmtr | Right side of the skull: most lateral point on fronto-malare suture |
| Glabella | glb | Most projecting midline point on the frontal bone above frontonasal suture. In juveniles with forward vaulted foreheads the most projecting point may not be the glabella. |
| Lambda | lam | Point where sagittal and lambdoidal sutures meet. If wormian bones are present, project the suture lines to their intersection point. |
| Left Mastoidale | mastl | Left mastoid process: point is located on the inferior end. |
| Right Mastoidale | mastr | Right mastoid process: point is located on the inferior end. |
| Nasion | nas | Midline intersection of the frontonasal suture and mid-sagittal plane. |
| Left Lower Orbital Border | obhi | Lower border of the left eye orbit: Measured as the maximum height from the upper to the lower orbital borders perpendicular to the horizontal axis of the orbit and using the middle of the inferior border as a fixed point |
| Left Upper Orbital Border | obhs | Upper left eye orbit: Upper border of the left eye orbit: Measured as the maximum height from the upper to the lower orbital borders perpendicular to the horizontal axis of the orbit and using the middle of the inferior border as a fixed point |
| Opisthion | ops | Midline point of the posterior foramen magnum margin where the mid-sagittal plan intersects. Opposite of basion. |
| Prosthion | pr / proHEST | Most anterior, midline point on the alveolar process of the maxilla between the central incisors. |
| Supspinale | ssp | The deepest point of the profile below the anterior nasal spine. |
| Left Nasomaxillary Suture Pinch | wnbl-simotic chord | Narrowest portion of the midline of the face to the left naso-maxillary suture. The minimum distance between wnbl-wnbr forms the simotic chord. |

| | | |
|---|---|---|
| Right Nasomaxillary Suture Pinch | wnbr-simotic chord | Narrowest portion of the midline of the face to the right naso-maxillary suture. The minimum distance between wnbl-wnbr forms the simotic chord. |
| Left Zygomaxillare | zygoml | Left side of skull: intersection of zygomaxillary suture and most medial masseter muscle attachment. |
| Right Zygomaxillare | zygomr | Right side of skull: intersection of zygomaxillary suture and most medial masseter muscle attachment. |
| Left Zygoorbitale | zygool | Left eye orbit: point of intersection between zygomaxillary suture and eye orbit. |
| Right Zygoorbitale | zygoor | Right eye orbit: point of intersection between zygomaxillary suture and orbit border. |
| Zygion | zygl | Left zygomatic: most lateral point on the zygomatic arch. (Point is determined by measuring bizygomatic breadth) |
| Zygion | zygr | Right zygomatic: most lateral point on the zygomatic arch. (Point is determined by measuring bizygomatic breadth) |
| Used for mastoidale: http://www.redwoods.edu/Instruct/AGarwin/anth_6_cranial-landmarks.htm | | |

References:

Howells, W.W. Cranial variation in man; a study by multivariate analysis of patterns of difference among recent human populations. Papers of the Peabody Museum of Archaeology and Ethnology Harvard University, Cambridge, Massachusetts, USA. Volume 67. Appendix B

Moore-Jansen, P., Jantz, R. 1994. Data collection procedures for forensic skeletal remains. Report of investigations / University of Tennessee, Dept. of Anthropology ; -- no. 48

http://www.redwoods.edu/Instruct/AGarwin/anth_6_cranial-landmarks.htm
http://www.cleber.com.br/howells.html
http://www.theapricity.com/snpa/gloss2.htm